analytical chemistry

Article

pubs.acs.org/ac

Dual-Targeted Nanocarrier Based on Cell Surface Receptor and Intracellular mRNA: An Effective Strategy for Cancer Cell Imaging and Therapy

Wei Pan, Huijun Yang, Tingting Zhang, Yanhua Li, Na Li,* and Bo Tang*

College of Chemistry, Chemical Engineering and Materials Science, Engineering Research Center of Pesticide and Medicine Intermediate Clean Production, Ministry of Education, Key Laboratory of Molecular and Nano Probes, Ministry of Education, Shandong Normal University, Jinan 250014, P.R. China

Supporting Information

ABSTRACT: Developing efficient methods for targeting cancer cells and encapsulating drugs coupled with activated release holds enormous potential for cancer cell imaging and therapy. Herein, a novel dual-targeted nanocarrier was developed on the basis of gold nanoparticles modified with a dense shell of synthetic oligonucleotides. The folic acid functionalized single-stranded DNA was designed to target the folate receptor on the cancer cell surface, and the molecular beacon was employed as drug carrier for activated release associated with intracellular tumor mRNA. Intracellular experiments indicated that the dual-targeted nanocarrier could be preferentially internalized into cancer cells due to the folate receptor targeting and release Doxorubicin (Dox) selectively in cancer cells because of the activated release with intracellular mRNA. The nanocarrier could reduce the dosage and greatly improve the therapeutic effect of drugs in cancer cells. Moreover, the nanocarrier can identify the changes of the express level of tumor mRNA and release Dox in a controlled manner in cancer cells, which would be beneficial for cancer therapy.

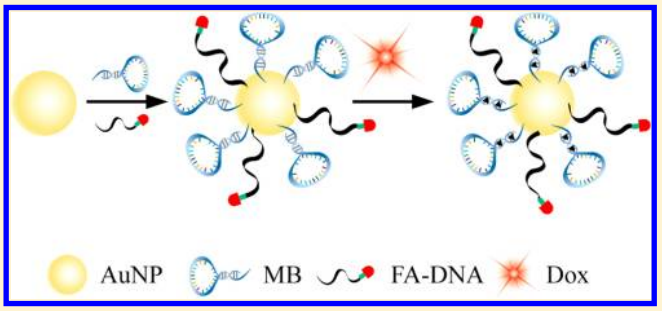

Cancer is one of the world's most devastating diseases, with several millions of deaths every year.[1] Typical treatments for cancer include surgery, radiation therapy, and chemotherapy. Chemotherapy is the use of antineoplastic drugs to destroy cancer cells, which may be given with a curative intent or may be employed to prolong life or alleviate symptoms as a palliative way. While chemotherapy is a quite effective treatment and the most commonly used for cancer, the therapeutic effect is often limited by the insolubility and instability of chemotherapeutic drugs and, more critically, by the nonspecific delivery and poor penetration of drugs into tumor sites.[2] Moreover, chemotherapeutic agents enter the bloodstream and distribute indiscriminately into all cells of the body, which also harms the healthy cells and results in many serious side effects during treatment. To address these issues, there is an urgent need to develop effective targeting platforms for cancer therapy.

In recent years, a number of nanocarriers have been exploited to deliver the chemotherapeutic drugs to the required pathological zone, in order to improve the solubility and stability, to extend the half-life, to improve the therapeutic index, and to reduce the immunogenicity.[3−6] Because of their small size and the leakiness of tumor blood vessels, the nanocarriers can preferentially accumulate in tumor tissues through the enhanced permeability and retention (EPR) effect,[7,8] which allows for passive tumor targeting. To further increase the selectivity and efficiency of drug delivery to cancer cells, active targeting of the nanocarriers can be achieved through the conjugation of specific targeting ligands, such as antibodies,[9] peptides,[10] carbohydrates,[11] and folic acid.[12] Folic acid possesses several advantages as a targeting agent, including lower molecular weight and immunogenicity than most antibodies, relatively high stability, and ease of synthesis.[13] The folic acid and folic acid−drug conjugates can bind the folate receptor (FR) on the cell surface with high affinity.[14,15] Significantly, the FR is a highly selective tumor marker overexpressed in some cancer cells. Using folate as the ligand, a variety of targeted nanocarriers has been successfully introduced for imaging and therapeutic applications.[16−19] However, the nanocarrier also can be internalized into normal cells via an endocytosis process. In this case, the chemotherapeutic drugs will be inevitably harmful for the normal cells due to the unexpected uptake. Hence, it is highly desirable to develop an effective nanocarrier that promotes the recognition and binding to cancer cells and encapsulates the cargo molecules coupled with intracellular activated release, which can destroy cancer cells selectively but not normal cells.

Herein, we present a novel and effective strategy to construct the dual-targeted nanocarrier, which combines active targeting to FR on the cell surface and activated release associated with

Received: May 8, 2013
Accepted: June 17, 2013
Published: June 17, 2013

intracellular tumor-related mRNA. The nanocarrier consists of gold nanoparticles modified by gold−thiol bond formation with a dense shell of synthetic oligonucleotides, which allows the good dispersibility in aqueous systems, high resistance to enzymatic degradation, and good biocompatibility.[20,21] The active targeting can be achieved by single-stranded DNA functionalized with folic acid. To encapsulate the drugs, the molecular beacon (MB) was utilized as the drug carrier for activated release because the MB has a unique oligonucleotide stem-loop configuration and can be designed to recognize some specific mRNA.[22−25] The Doxorubicin (Dox) molecules can intercalate into the double-stranded GC or CG sequences of the stem regions in MB,[26,27] leading to the quench of the fluorescence and the decrease of the cytotoxicity for Dox. The loop sequences of the MB contained 17-base recognition element to TK1 mRNA. TK1 mRNA is associated with cell division and proposed to be an important marker of tumor growth.[28,29] In the presence of DNA or RNA targets, the loop of MB hybridized with the complementary target sequences by forming longer and more stable duplexes, causing the opening of MB and the release of Dox molecules. Then, the fluorescence and cytotoxicity of Dox were recovered, and the Dox was released controllably in a target concentration-dependent manner. The details of this strategy are described in Figure 1.

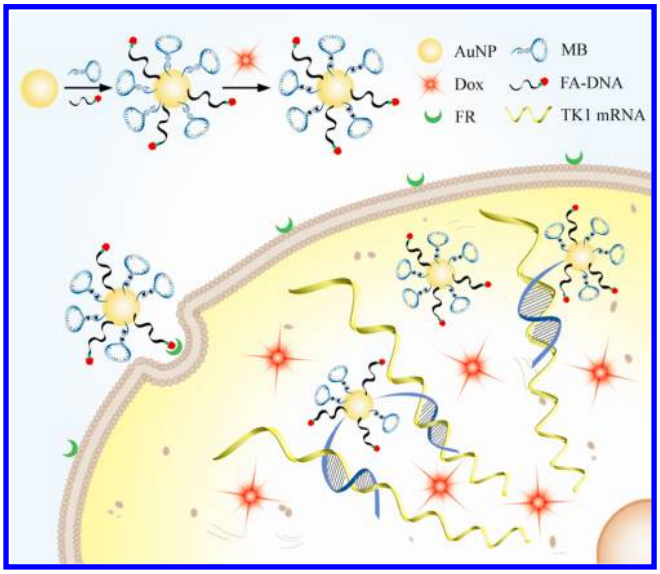

Figure 1. Schematic illustration of the design and cell internalization of dual-targeted nanocarrier.

RESULTS AND DISCUSSION

The folic acid modified single-stranded DNA (5′-FA-ATGA-AGTGTCCAGTGTAATGAAAAAA-$(CH_2)_3$-SH-3′) was designed to target the FR on the cancer cell surface, and the MB (5′-CGACGCCAGGGAGAACAGAAACCGTCGAAA-AAA-$(CH_2)_3$-SH-3′) (underlined letters represent the stem sequence) was employed to target the intracellular TK1 mRNA. To determine the amounts of Dox molecules loaded in one MB, we measured the Dox fluorescence intensity by incubating Dox (0.2 μM) with different concentrations of MB. Sequential decreases in the fluorescence intensity of Dox were observed with the increase of MB concentrations (Figure S1, Supporting Information). The maximal quenching of the Dox fluorescence was observed when the MB concentration reached 0.1 μM, and the fluorescence intensity did not show an obvious change with the further addition of MB (0.12 μM). It indicated that two Dox molecules could intercalate into a single MB, which was consistent with the design of two double-stranded GC sequences in the stem of the MB (Scheme S1, Supporting Information).

Gold nanoparticles (AuNPs) with diameter of 13 nm were used for the nanocarrier because it has been reported that AuNPs with this size are an efficient quencher and can be densely functionalized with oligonucleotides.[30,31] The dual-targeted nanocarrier was then synthesized by mixing the AuNPs and different molar ratios of the folic acid modified single-stranded DNA (FA-DNA) and MB (0:10, 0.25:9.75, 0.5:9.5, 1:9, and 2:8). On the basis of the previous protocol,[32] each AuNP was calculated to carry about 52 MBs (0:10), 2 FA-DNAs and 51 MBs (0.25:9.75), 8 FA-DNAs and 46 MBs (0.5:9.5), 13 FA-DNAs and 44 MBs (1:9), and 31 FA-DNA and 33 MBs (2:8) for each ratio, respectively. Details of the characterization are provided in the Supporting Information and Figure S2. In order to make sure that there is enough FA-DNA to target the FR on the cancer cell surface and maximize the loaded Dox molecules for killing the cancer cells, a molar ratio of 1:9 was chosen in the following experiments.

The TEM images of AuNPs and nanocarrier were shown in Figure S3, Supporting Information. The border of the AuNPs was clear while that of the nanocarrier was ambiguous, which suggested the successful assembly of DNA on the surface of AuNPs. The UV−vis absorption spectra showed the maximum absorption of the AuNPs was at 518 nm, and it was red-shifted to 524 nm for the nanocarrier, which further confirmed the AuNPs were successfully functionalized with DNA (Figure S4, Supporting Information).

The release of Dox molecules from nanocarrier was performed by the hybridization experiments with the perfectly matched DNA target and mismatched DNA targets under the identical condition. Kinetic studies showed that the nanocarrier responded rapidly to the perfectly matched DNA target within 5 min (Figure S5, Supporting Information). The fluorescence intensity of Dox increased with the increase of the DNA target concentrations from 0 to 200 nM, thus indicating that the hybridization of nanocarrier and DNA targets forced the MB to open and released the Dox molecules. Moreover, the fluorescence intensity of Dox is correlated positively with the concentration of DNA targets in a concentration-dependent manner (Figure 2). The selectivity of the nanocarrier was shown in Figure S6, Supporting Information. The results revealed that the nanocarrier specifically released the Dox

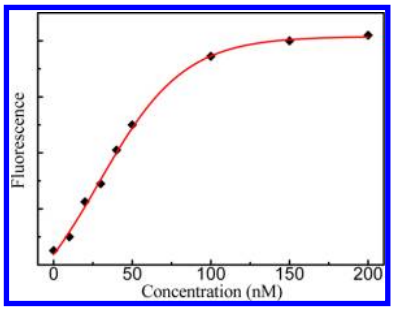

Figure 2. Fluorescence curves for the nanocarrier (1 nM) in the presence of various concentrations of DNA target (0, 10, 20, 30, 40, 50, 100, 150, and 200 nM) measured with 490 nm excitation.

dx.doi.org/10.1021/ac401405n | Anal. Chem. 2013, 85, 6930−6935

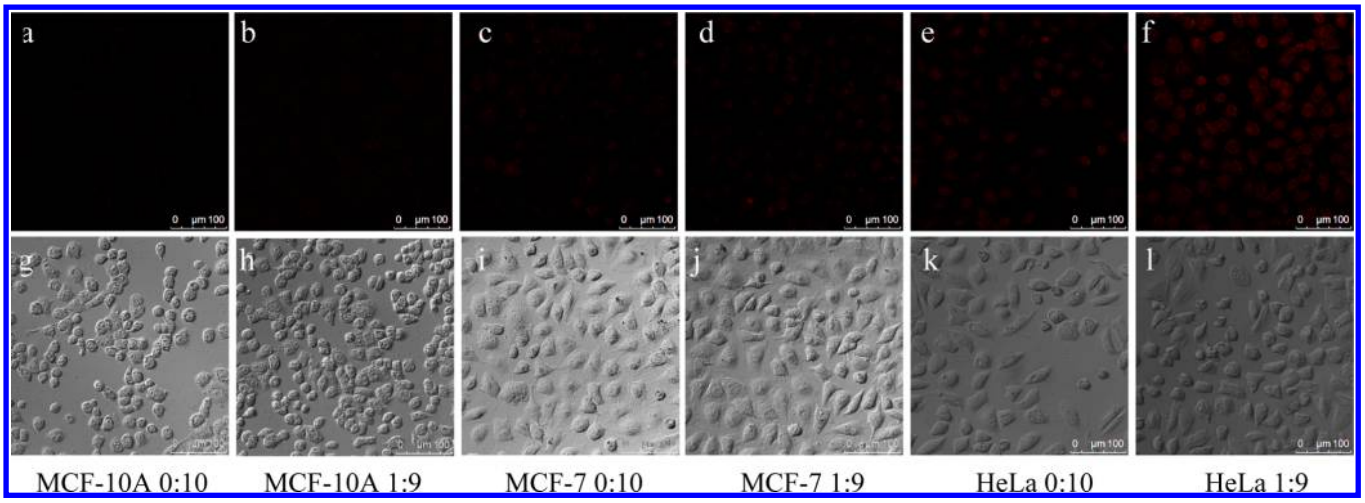

Figure 3. Intracellular imaging of Dox in MCF-7, MCF-10A, and HeLa cells under CLSM. The cells were incubated with the nanocarriers (0:10 and 1:9) for 4 h at 37 °C. The fluorescence of Dox was recorded with 488 nm excitation. Scale bars are 100 μm.

molecules when bound to its perfectly matched DNA target and generated a 5- to 6-fold higher fluorescent signal compared with other targets.

The stability of the nanocarrier was investigated by time-dependent fluorescence change at room temperature. Less than 3% Dox was released after 30 days (Figure S7, Supporting Information), which suggested the nanocarrier performed well in resisting the unexpected release of drug molecules. Nuclease stability is a key property of the nanocarrier for imaging and therapeutic applications when used in living cells. The nuclease stability of the nanocarrier was evaluated with enzyme deoxyribonuclease I (DNase I), a common endonuclease,[20] under physiological condition with fluorescence spectroscopic analysis. The results showed that the fluorescence intensity of the nanocarrier treated with DNase I was not obviously changed compared with the case without DNase I (Figure S8, Supporting Information). However, the fluorescence intensity of the two solutions was all enhanced greatly after hybridization with the DNA targets (Figure S8, inset, Supporting Information). It demonstrated the nanocarrier possessed high resistance to nuclease and further confirmed that the release of Dox was indeed due to the hybridization of the nanocarrier and targets instead of nuclease degradation.

To evaluate the targeting effect of the nanocarrier in living cells, three different cell lines were chosen: cervical cancer cell line (HeLa) where folate receptor and TK1 mRNA were all overexpressed, human breast cancer cell line (MCF-7) where only TK1 mRNA was overexpressed, and normal immortalized human mammary epithelial cell line (MCF-10A) where folate receptor and TK1 mRNA were all not overexpressed.[33−35] The intracellular uptake efficiency of the nanocarrier in different cells was determined using an approach based on inductively coupled plasma atomic emission spectroscopy (ICP-AES).[36,37] Figure S9, Supporting Information, showed that the nanocarrier could be taken up in all the three cells, and the uptake amounts of the nanocarrier in single HeLa cell were much more than that in MCF-7 and MCF-10A, which is consistent with the fact that the FR was overexpressed in HeLa but not in MCF-7 and MCF-10A. When the nanocarriers with different ratios of FA-DNA and MB (0:10, 0.25:9.75, 0.5:9.5, and 1:9) were incubated with HeLa cells, the uptake amounts of the nanocarrier in a single HeLa cell increased with the increase of the FA-DNA (Figure S10, Supporting Information). The results suggested that the uptake amounts of nanocarrier in FR-overexpressed cancer cells could be increased remarkably when the nanocarrier functionalized with FA-DNA.

For the application of nanocarrier for targeted delivery of Dox, an intracellular release experiment was carried out in the three cell lines mentioned above. After MCF-10A cells were incubated with the nanocarrier with FA-DNA (1:9, the loaded Dox concentration is 0.1 μM) and without FA-DNA (0:10, the loaded Dox concentration is 0.1 μM) for 4 h at 37 °C, a very faint fluorescence signal was observed under confocal laser scanning microscopy (CLSM) (Figure 3a,b). When MCF-7 cells were incubated under the same condition, both of the fluorescence signals became higher (Figure 3c,d), indicating that the TK1 mRNA expression was much higher in MCF-7 than in MCF-10A. A red fluorescence signal was also observed under CLSM in HeLa cells after being incubated with the nanocarrier (0:10), which was similar with the case in MCF-7 cells (Figure 3e). Interestingly, after HeLa cells were incubated with the nanocarrier (1:9), the red fluorescent signal was much stronger than other cases (Figure 3f), indicating that the nanocarrier could release more Dox molecules because the FR and TK1 mRNA in HeLa were both overexpressed. The results of flow cytometry also showed that the fluorescent signal increased in an order of MCF-10A, MCF-7, and HeLa cells when incubated with the nanocarrier (1:9) under the same condition (Figure S11, Supporting Information), which was consistent with the confocal imaging results. Real-time reverse transcription-PCR (RT-PCR) results further verified that the relative levels of TK1 in HeLa and MCF-7 were much higher than in MCF-10A (Figure S12, Supporting Information). To confirm the targeting effect of the dual-targeted nanocarrier when the normal cells and cancer cells coexisted, the coincubation experiment of HeLa and MCF-10A was performed. As shown in Figure 4, after HeLa cells and MCF-10A cells were incubated with the nanocarrier (1:9), a strong red fluorescent signal was only observed in HeLa cells, while the fluorescent signal was very faint in MCF-10A cells. These results demonstrated that the dual-targeted nanocarrier could be preferentially internalized into specific cancer cells due to the FR targeting and release Dox molecules selectively in cancer cells because of the activated release with intracellular TK1 mRNA.

dx.doi.org/10.1021/ac401405n | *Anal. Chem.* 2013, 85, 6930−6935

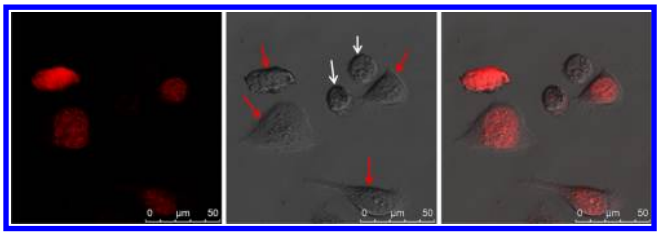

Figure 4. Intracelluar imaging of Dox under CLSM when the HeLa and MCF-10A cells were coincubated with the nanocarrier (1:9) for 4 h at 37 °C. The red arrows point at the HeLa cells, and the white arrows point at the MCF-10A cells. Scale bars are 50 μm.

To evaluate the therapeutic effect of the nanocarrier, an MTT (3-(4,5-dimethylthiazol-2-yl)-2,5-diphenylte-trazolium bromide) assay was performed. The absorbance of MTT at 490 nm is dependent on the degree of activation of the cells. Then, the cell viability was expressed by the ratio of absorbance of the treated cells (incubated with the nanocarrier or free Dox) to that of the untreated cells. As shown in Figure 5a, the cell viability was about 95% when the nanocarriers (0:10 and 1:9, the loaded Dox concentrations are both 0.1 μM) were incubated with the MCF-10A cells, which was higher than when an equal amount of Dox was added (0.1 μM). It indicated that the nanocarrier indeed performed well to prevent the Dox molecules from unexpected release in normal cells. Figure 5b showed that an obvious decrease in the cell viability (about 80%) was observed after the nanocarriers (0:10 and 1:9) were incubated with the MCF-7 cells, which was lower than when an equal amount of Dox was added and nearly equal to ten times of Dox added, suggesting that the nanocarrier could release the Dox and kill cancer cells owing to the intracellular activated release associated with TK1 mRNA. Then, HeLa cells were treated with nanocarriers (0:10 and 1:9) under the same condition. After being incubated with the nanocarrier (0:10), the cell viability was similar to that of the MCF-7 cells. Notably, the cell viability decreased sharply to about 60% when the nanocarrier (1:9) was incubated with the HeLa cells. It demonstrated that the dual-targeted nanocarrier exhibited better therapeutic effect toward specific cancer cells than single-targeted nanocarrier. Moreover, the therapeutic effect of the current nanocarrier was much better than when ten times of Dox was added, indicating the nanocarrier could reduce the dosage and greatly improve the therapeutic effect of drugs in cancer cells (Figure 5c). These results were in agreement with the intracellular imaging experiment, which further confirmed that the dual-targeted nanocarrier performed well compared with single-targeted nanocarrier as well as free drugs in cancer cell therapy.

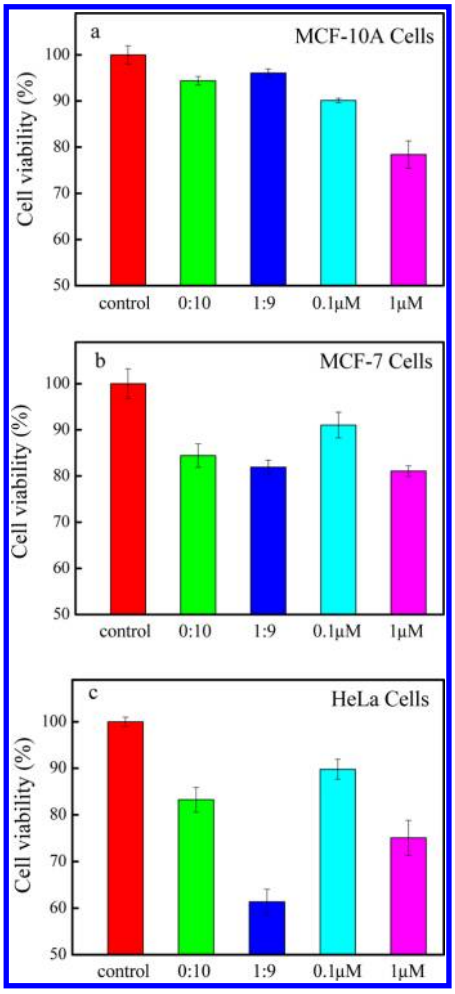

Figure 5. MTT assay of three types of cells. The cells were incubated with nanocarriers (0:10 and 1:9, the loaded Dox concentrations are both 0.1 μM) and free Dox (0.1 and 1 μM) for 4 h and then cultured with DMEM for 24 h at 37 °C. (a) MCF-10A cells; (b) MCF-7 cells; (c) HeLa Cells.

The relative expression level of tumor mRNA is different in cancer cells and normal cells or in the various stages of tumor progression. It is critical for the nanocarrier to release the drugs according to the relative expression level of tumor mRNA during treatment in living cells. We investigated the ability of the nanocarrier to release the Dox when the mRNA expression levels were different in HeLa cells. The previous report showed that β-estradiol could induce up-regulation of TK1 mRNA expression and tamoxifen could induce down-regulation of TK1 mRNA expression.[38,39] HeLa cells were paralleled and divided into three groups. One group was treated with β-estradiol for 48 h to increase the TK1 mRNA expression, and another one was treated with tamoxifen for 48 h to decrease the TK1 mRNA expression. The untreated one served as a control. Then, the treated and untreated cells were incubated with the nanocarrier (1:9, the loaded Dox concentration is 0.1 μM). As shown in Figure 6, the fluorescence intensity was higher in the β-estradiol treated cells and lower in the tamoxifen treated cells compared with the untreated cells. The results of flow cytometry were consistent with the confocal imaging results (Figure S13, Supporting Information). RT-PCR results further confirmed that β-estradiol increased the level of TK1 mRNA and tamoxifen decreased the level of TK1 mRNA in HeLa cells (Figure S14, Supporting Information). Furthermore, the MTT assay indicated that the cell survival decreased when the mRNA expression levels increased in HeLa cells. These results revealed that the fluorescence intensity correlated positively with the levels of tumor mRNA expression and the release of Dox for the nanocarrier is dependent on the levels of tumor mRNA in living cells.

CONCLUSION

In summary, we have developed a novel dual-targeted nanocarrier based on cell surface receptor and intracellular mRNA, which is effective for cancer cell imaging and therapy. The nanocarrier exhibits high specificity, good stability, and biocompatibility. Intracellular experiments indicated that the

dx.doi.org/10.1021/ac401405n | Anal. Chem. 2013, 85, 6930−6935

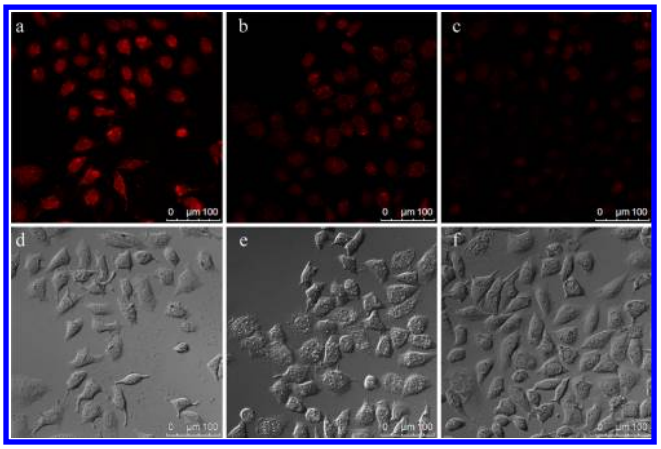

Figure 6. Intracellular imaging of Dox for the different levels of TK1 mRNA under CLSM. The treated and untreated HeLa cells were incubated with the nanocarrier for 4 h at 37 °C. The middle panels (b, e) were the control group, the left panels (a, d) were the β-estradiol-treated group, and the right panels (c, f) were the tamoxifen-transduced group. Images a, b, and c were obtained with excitation at 488 nm; images d, e, and f were the bright-field images of a, b, and c. Scale bars are 100 μm.

dual-targeted nanocarrier could be effectively internalized into the cancer cells by active targeting to the folate receptor and release the Dox molecules due to the activated release coupled with intracellular TK1 mRNA. The dosage of chemotherapeutic drugs could be noticeably reduced, and the therapeutic effect could be greatly enhanced in cancer cells when encapsulated with the nanocarrier. Compared with traditional single-targeted nanocarriers, the current nanocarrier performed well in protecting the normal cells and killing cancer cells effectively. Moreover, the nanocarrier can identify the changes of the expression level of the tumor mRNA and release Dox in a controlled manner in cancer cells, which would be beneficial for cancer therapy. We anticipate that the nanocarrier will provide new opportunities to improve the efficacy of cancer cell imaging and therapy with cell surface receptors and intracellular cancer markers.

EXPERIMENTAL SECTION

Preparation of the Nanocarrier. The procedure for coating gold nanoparticles with MB and folic acid modified single-stranded DNA (FA-DNA) was adapted from the reported protocol,[30] which was based on the gold−thiol interaction between the gold lattice and thiol functionalized oligonucleotides. Different molar ratios of the FA-DNA and MB (0:10, 0.25:9.75, 0.5:9.5, 1:9, and 2:8) were mixed and added to a solution of AuNPs (3 nM) and shaken overnight. After 12 h, phosphate buffer (0.1 M, pH = 7.4) was added to the mixture to achieve 0.01 M phosphate concentration and the NaCl concentration of the mixture was slowly increased to 0.1 M over an 8 h period. The solution containing the nanocarrier was centrifuged (13 500*g*, 30 min) and resuspended in phosphate buffer saline (PBS) for three times. Then, the nanocarrier was sterilized using a 0.22 μm acetate syringe filter and resuspended in PBS as stock solution at 4 °C. The nanocarrier was diluted to a certain concentration for use in all subsequent experiments. The concentration of nanocarrier was determined by measuring the extinction of AuNPs at 524 nm (ε = 2.7 × 10^8 L mol^{-1} cm^{-1}).

Release of Dox from the Nanocarrier Induced by DNA Target. The obtained nanocarrier (1:9) was diluted to a concentration of 1 nM in buffer (10 mM Tris·HCl of pH 7.4, 100 mM KCl, 1 mM $MgCl_2$) and treated with a complementary DNA target with an increasing concentration (concentration of 0, 10, 20, 30, 40, 50, 100, 150, and 200 nM). After a 30 min incubation, the fluorescence spectra were obtained in the range from 505 to 650 nm by use of the maximal excitation wavelength at 490 nm. In kinetic studies, DNA target of 200 nM was employed. The kinetic study was performed at 37 °C, and the fluorescence intensity was measured with 490 nm excitation wavelength.

Confocal Fluorescence Imaging. In a comparative experiment of cancer cells and normal cells, all cells were plated on chamber slides for 24 h. Then, the nanocarriers (0:10 and 1:9) in which the loaded Dox concentrations are both 0.1 μM were, respectively, delivered into MCF-10A, MCF-7, and HeLa cells in DMEM culture medium at 37 °C in 5% CO_2 for 4 h. The cells were examined by confocal laser scanning microscopy (CLSM) with 488 nm excitation.

In the experiments for coincubation experiments, MCF-10A cells were plated on chamber slides for 6 h, and then, equivalent HeLa cells were added on the same chamber slides for another 18 h. After that, the nanocarrier (1:9) with the Dox concentration of 0.1 μM was delivered into the coincubated cells. Other steps were performed as described above.

In the experiments for the expression levels of tumor mRNA, one group of HeLa cells was treated with β-estradiol (10^{-8} mol/L) and the other group of HeLa cells was treated with tamoxifen (10^{-6} mol/L) for 48 h. One group of HeLa cells without regulation served as the control. Other steps were performed as described above using the nanocarrier (1:9, the loaded Dox concentration of 0.1 μM).

MTT Assay. MCF-10A, MCF-7, and HeLa cells were cultured in 96-well microtiter plates and incubated at 37 °C in 5% CO_2 for 24 h. After the original medium was removed, the cells were incubated with nanocarrier (0:10 and 1:9, the loaded Dox concentrations are both 0.1 μM) and free Dox (0.1 μM and 1 μM) for 4 h. Then, the cells were washed with PBS for three times. After that, the cells were cultured with DMEM at 37 °C for 24 h. Next, 150 μL of MTT solution (0.5 mg/mL in PBS) was added to each well. After 4 h, the remaining MTT solution was removed, and 150 μL of DMSO was added to each well to dissolve the formazan crystals. The absorbance was measured at 490 nm with a RT 6000 microplate reader. The cells incubated without nanocarrier served as the control. Then, the Hela cells were divided into four groups; one group of HeLa cells was treated with β-estradiol (10^{-8} mol/L), and one group of HeLa cells was treated with tamoxifen (10^{-6} mol/L) for 48 h. The other two groups of HeLa cells were without any treatment. One group of untreated Hela cells were incubated with nanocarrier (1:9, without loading of Dox) and the other three groups of cells were incubated with nanocarrier (1:9, the loaded Dox concentration of 0.1 μM). Other steps were performed as described above. The cells without treatment and incubated without nanocarrier served as the control.

ASSOCIATED CONTENT

Supporting Information

Experimental details, supporting table, and supporting figures. This material is available free of charge via the Internet at http://pubs.acs.org.

dx.doi.org/10.1021/ac401405n | *Anal. Chem.* 2013, 85, 6930−6935

AUTHOR INFORMATION

Corresponding Author

*E-mail: lina@sdnu.edu.cn (N.L.); tangb@sdnu.edu.cn (B.T.).

Notes

The authors declare no competing financial interest.

ACKNOWLEDGMENTS

This work was supported by 973 Program (2013CB933800), National Natural Science Foundation of China (21227005, 21035003, 21105059), Specialized Research Fund for the Doctoral Program of Higher Education of China (20113704130001), Shandong Distinguished Middle-Aged and Young Scientist Encourage and Reward Foundation (BS2011CL037), and Program for Changjiang Scholars and Innovative Research Team in University.

REFERENCES

(1) Jemal, A.; Bray, F.; Center, M. M.; Ferlay, J.; Ward, E.; Forman, D. *CA Cancer J. Clin.* **2011**, *61*, 69−90.

(2) Ding, M.; Li, J.; He, X.; Song, N.; Tan, H.; Zhang, Y.; Zhou, L.; Gu, Q.; Deng, H.; Fu, Q. *Adv. Mater.* **2012**, *24*, 3639−3645.

(3) Peer, D.; Karp, J. M.; Hong, S.; Farokhzad, O. C.; Margalit, R.; Langer, R. *Nat. Nanotechnol.* **2007**, *2*, 751−760.

(4) Davis, M. E.; Chen, Z.; Shin, D. M. *Nat. Rev. Drug Discovery* **2008**, *7*, 771−782.

(5) Zhang, L.; Gu, F. X.; Chan, J. M.; Wang, A. Z.; Langer, R. S.; Farokhzad, O. C. *Clin. Pharmacol. Ther.* **2008**, *83*, 761−769.

(6) Petros, R. A.; DeSimone, J. M. *Nat. Rev. Drug Discovery* **2010**, *9*, 615−627.

(7) Maeda, H.; Fang, J.; Inutsuka, T.; Kitamoto, Y. *Int. Immunopharmacol.* **2003**, *3*, 319−328.

(8) Torchilin, V. *Adv. Drug Delivery Rev.* **2011**, *63*, 131−135.

(9) Barth, B. M.; Altinoglu, E. I.; Shanmugavelandy, S. S.; Kaiser, J. M.; Crespo-Gonzalez, D.; DiVittore, N. A.; McGovern, C.; Goff, T. M.; Keasey, N. R.; Adair, J. H.; Loughran, T. P.; Claxton, D. F.; Kester, M. *ACS Nano* **2011**, *5*, 5325−5337.

(10) Hah, H. J.; Kim, G.; Koo, Y.-E. L.; Orringer, D. A.; Sagher, O.; Philbert, M. A.; Kopelman, R. *Macromol. Biosci.* **2011**, *11*, 90−99.

(11) Gary-Bobo, M.; Mir, Y.; Rouxel, C.; Brevet, D.; Basile, I.; Maynadier, M.; Vaillant, O.; Mongin, O.; Blanchard-Desce, M.; Morere, A.; Garcia, M.; Durand, J.-O.; Raehm, L. *Angew. Chem., Int. Ed.* **2011**, *50*, 11425−11429.

(12) Fan, N.-C.; Cheng, F.-Y.; Ho, J.-A. A.; Yeh, C.-S. *Angew. Chem., Int. Ed.* **2012**, *51*, 8806−8810.

(13) Wang, X.; Li, J.; Wang, Y.; Cho, K. J.; Kim, G.; Gjyrezi, A.; Koenig, L.; Giannakakou, P.; Shin, H. J. C.; Tighiouart, M.; Nie, S.; Chen, Z.; Shin, D. M. *ACS Nano* **2009**, *3*, 3165−3174.

(14) Sudimack, J.; Lee, R. J. *Adv. Drug Delivery Rev.* **2000**, *41*, 147−162.

(15) Leamon, C. P.; Reddy, J. A. *Adv. Drug Delivery Rev.* **2004**, *56*, 1127−1141.

(16) Dhar, S.; Liu, Z.; Thomale, J.; Dai, H.; Lippard, S. J. *J. Am. Chem. Soc.* **2008**, *130*, 11467−11476.

(17) Zhang, Z.; Lee, S. H.; Feng, S.-S. *Biomaterials* **2007**, *28*, 1889−1899.

(18) Rosenholm, J. M.; Meinander, A.; Peuhu, E.; Niemi, R.; Eriksson, J. E.; Sahlgren, C.; Lindén, M. *ACS Nano* **2009**, *3*, 197−206.

(19) Mizusawa, K.; Takaoka, Y.; Hamachi, I. *J. Am. Chem. Soc.* **2012**, *134*, 13386−13395.

(20) Seferos, D. S.; Prigodich, A. E.; Giljohann, D. A.; Patel, P. C.; Mirkin, C. A. *Nano Lett.* **2009**, *9*, 308−311.

(21) Zhang, X.-Q.; Xu, X.; Lam, R.; Giljohann, D.; Ho, D.; Mirkin, C. A. *ACS Nano* **2011**, *5*, 6962−6970.

(22) Bonnet, G.; Tyagi, S.; Libchaber, A.; Kramer, F. R. *Proc. Natl. Acad. Sci. U. S. A.* **1999**, *96*, 6171−6176.

(23) Dubertret, B.; Calame, M.; Libchaber, A. J. *Nat. Biotechnol.* **2001**, *19*, 365−370.

(24) Song, S.; Liang, Z.; Zhang, J.; Wang, L.; Li, G.; Fan, C. *Angew. Chem., Int. Ed.* **2009**, *48*, 8670−8674.

(25) Song, S.; Qin, Y.; He, Y.; Huang, Q.; Fan, C.; Chen, H.-Y. *Chem. Soc. Rev.* **2010**, *39*, 4234−4243.

(26) Fan, P.; Suri, A. K.; Fiala, R.; Live, D.; Patel, D. J. *J. Mol. Biol.* **1996**, *258*, 480−500.

(27) Qiao, G.; Zhuo, L.; Gao, Y.; Yu, L.; Li, N.; Tang, B. *Chem. Commun.* **2011**, *47*, 7458−7460.

(28) Chen, C. C.; Chang, T. W.; Chen, F. M.; Hou, M. F.; Hung, S. Y.; Chong, I. W.; Lee, S. C.; Zhou, T. H.; Lin, S. R. *Oncology* **2006**, *70*, 438−446.

(29) Broet, P.; Romain, S.; Daver, A.; Ricolleau, G.; Quillien, V.; Rallet, A.; Asselain, B.; Martin, P. M.; Spyratos, F. *J. Clin. Oncol.* **2001**, *19*, 2778−2787.

(30) Mirkin, C. A.; Letsinger, R. L.; Mucic, R. C.; Storhoff, J. J. *Nature* **1996**, *382*, 607−609.

(31) Li, N.; Chang, C.; Pan, W.; Tang, B. *Angew. Chem., Int. Ed.* **2012**, *51*, 7426−7430.

(32) Demers, L. M.; Mirkin, C. A.; Mucic, R. C.; Reynolds, R. A.; Letsinger, R. L.; Elghanian, R.; Viswanadham, G. *Anal. Chem.* **2000**, *72*, 5535−5541.

(33) Zheng, X.; Kelley, K.; Yan, W.; Dorn, T.; Ratnam, M. *Mol. Cell. Biol.* **2003**, *23*, 2202−2212.

(34) Sonvico, F.; Mornet, S.; Vasseur, S.; Dubernet, C.; Jaillard, D.; Degrouard, J.; Hoebeke, J.; Duguet, E.; Colombo, P.; Couvreur, P. *Bioconjugate Chem.* **2005**, *16*, 1181−1188.

(35) Chen, H.; Ahn, R.; Van den Bossche, J.; Thompson, D. H.; O'Halloran, T. V. *Mol. Cancer Ther.* **2009**, *8*, 1955−1963.

(36) Chithrani, B. D.; Ghazani, A. A.; Chan, W. C. W. *Nano Lett.* **2006**, *6*, 662−668.

(37) Freese, C.; Gibson, M. I.; Klok, H. A.; Unger, R. E.; Kirkpatrick, C. J. *Biomacromolecules* **2012**, *13*, 1533−1543.

(38) Kasid, A.; Davidson, N. E.; Gelmann, E. P.; Lippman, M. E. *J. Biol. Chem.* **1986**, *261*, 5562−5567.

(39) Foekens, J. A.; Romain, S.; Look, M. P.; Martin, P. M.; Klijn, J. G. M. *Cancer Res.* **2001**, *61*, 1421−1425.